Title
THE PRODUCTION OF CHARGED PI MESONS BY NEUTRONS ON OXYGEN

Author
Ford, Franklin C.

Publication Date
1953-03-20

UNIVERSITY OF CALIFORNIA — BERKELEY

RADIATION LABORATORY

DISCLAIMER

UCRL-2148
Unclassified-Physics Distribution

UNIVERSITY OF CALIFORNIA

Radiation Laboratory

Contract No. W-7405-eng-48

THE PRODUCTION OF CHARGED PI MESONS BY NEUTRONS ON OXYGEN

Franklin C. Ford

(Thesis)

March 20, 1953

Berkeley, California

TABLE OF CONTENTS

THE PRODUCTION OF CHARGED PI MESONS BY NEUTRONS ON OXYGEN

Franklin C. Ford

ABSTRACT

Charged mesons were produced in oxygen gas in a cloud chamber bombarded by high-energy neutrons from a LiD target placed in the 340 Mev proton beam of the 184-inch cyclotron. The postulated reactions producing the negative pions are:

$$n + n \longrightarrow n + p + \pi^-$$
$$\text{or } d + \pi^-$$
$$n + p \longrightarrow p + p + \pi^-$$

and the reaction for the positive pions is:

$$n + p \longrightarrow n + n + \pi^+$$

The particles of the disintegration were identified by curvature and relative ionization and by characteristic track endings. As many as seven tracks were associated with a single star. Measurements of the energy and momentum of the disintegration fragments gave a minimum energy for the neutrons producing mesons. A weighting factor was computed for each meson which corrected for tracks too slanted to be measured. The angular distribution of the pions was obtained for the laboratory frame and for a special center of mass frame. The fast particles associated with each meson event were identified and tabulated for energy and angle. An absolute cross section of 4.4 millibarns for meson production by the neutron beam was established by normalizing with respect to ordinary star production for neutron energies above 280 Mev, and by normalizing with respect to the n-p cross section using a beam monitor to relate the data of two cloud chamber experiments.

THE PRODUCTION OF CHARGED PI MESONS BY NEUTRONS ON OXYGEN

Franklin C. Ford

INTRODUCTION

Experiments involving the production of pi mesons may be expected to indicate which features of present meson theories are qualitatively correct and to furnish quantitative checks with which any future meson theory must agree. Pi mesons are important because they are intimately associated with the fundamental problem of nuclear physics--the problem of nuclear forces. The cloud chamber is particularly adapted to the study of meson production involving neutrons on nuclei as it presents the ultimate in "thin" targets resulting in the best possible view of the associated particles in the reaction. The energetics of the collisions still remain somewhat of a mystery, but the general participation of the nucleus can be observed to a higher degree than by other experimental means. It is always hoped that the experimental results will contain striking features from which the meson-nucleon interaction may be deduced directly.

The charged particles ejected from nuclei bombarded by high energy neutrons have been studied[1,2,3] in a number of experiments and the results indicate that the collision process for high energies is predominantly the interaction of the bombarding particle with an individual nucleon rather than with the nucleus as a whole. The theory as outlined by Goldberger[4] predicts the production of fast particles in the forward direction and low energy particles emitted more or less isotropically, and when sufficiently high energies are reached the production of pions becomes possible.

Gardner and Lattes were the first to observe the production of mesons in the laboratory using high energy alpha-particles to bombard targets. When neutrons are used as the bombarding particle, the problem of generating a beam with a reasonably narrow high-energy peak arises. A suitable neutron beam was obtained by bombarding a LiD target[5] with 340 Mev protons. With any other target the background

in a cloud chamber due to the low energy events is too great for a reasonable meson production rate. Mesons produced by neutrons bombarding argon gas in a cloud chamber were first observed by Hartsough, Hayward, and Powell.[6] However at that time the copper target used in the cyclotron produced so many lower energy neutrons that the high background of other events in the chamber made a detailed study of the pion production impractical. One technique used to avoid background in another experiment, using neutrons on carbon,[7] employed a time of flight measurement for the pions; but only a limited part of the pion spectrum can be studied with such methods at present. The usual technique in charged meson studies makes use of nuclear emulsions embedded in absorbers and magnetic separation to sort out the mesons formed at desired angles.[8]

The splitting up of a nucleus is referred to as a star when two or more charged particles are visible in a cloud chamber or nuclear emulsion. Neutron-induced stars are particularly suited for study with a cloud chamber. A star experiment using 90 Mev neutrons was carried out by Tracy and Powell,[9] and the techniques developed by them for analyzing the fragments of the stars were extended by Peter Tannenwald[10] for study of neutron-induced events in helium. This same basic technique of track identification has been applied in the present study. The low cross section for the production of pions in hydrogen, helium, and monatomic carbon (such as methane) made it necessary to use a high-pressure cloud chamber for studies involving meson production by neutrons on these nuclei. Oxygen gas gives sufficient production to permit its use at atmospheric pressure. An experiment using deuterium in a ten atmosphere cloud chamber[11] is now in progress.

EXPERIMENTAL PROCEDURE

Apparatus

The neutrons produced by bombarding a one-inch thick LiD target with 340 Mev protons were collimated outside the concrete shielding of the 184-inch Berkeley cyclotron by means of a rectangular copper collimator three feet long passing a beam three inches wide and one inch high (see Figs. 1, 2, and 3). The neutrons entered the 22-inch Wilson cloud chamber[13] through a three mill copper foil window 5 x 1 inch, and passed out through a similar window to reduce back-scattering from the exit wall of the chamber. The bottom of the chamber consisted of a half-inch thick homalite disk which moved vertically and was controlled by a pantograph which kept it horizontal during the expansions.

Gelatin containing a black dye covered the disk to a depth of 1/16 inch to provide a black background for photographing the tracks. General Electric FT422 flash tubes were used on either side of the chamber and gave uniform illumination over 2 1/2 in. of the 3 1/2 in. high chamber.[14] Each lamp was flashed by discharging 256 microfarad condensers charged to 1700 volts through it.

Operation

The cloud chamber was operated in a pulsed magnetic field of 22,000 gauss which was energized by a 150 h.p. mine-sweeper generator. The field requires about 2.5 sec. to attain its maximum value, where it remains steady for about 0.15 sec. before being turned off. The cycle of operation, repeated once a minute, is as follows: the current is turned on in advance so that its maximum coincides with the expansion of the chamber. The cyclotron beam is pulsed through the chamber at the instant the diaphragm hits bottom, and the lights are flashed about 0.04 sec. after the beam signal. The current which passes through the magnet is recorded with each picture through a third lens which views the magnet current meter. The chamber is kept at constant temperature by means of a temperature-controlled circulating water system. A clearing field of about 60 volts is turned off prior to expansion of the chamber and turned on again after the lights have flashed.

The chamber was filled with oxygen gas to a total pressure of 86 cm Hg in the expanded position. Of this pressure 1.8 cm was due to the partial water vapor pressure from the gelatin. The chamber was then compressed to a total pressure of 111.0 cm representing an expansion ratio of around 29 percent.

Photography

A specially constructed camera was mounted on a light-tight crown 27 in. above the top glass of the chamber. The pictures were taken through a pair of Leica lenses at f 6.3 on Eastman Linagraph Ortho film in 100 foot strips 1.80 in. wide. Life-size reprojections, which duplicated the geometry of the camera optical system and employed the camera lenses, were used for measuring the tracks. Western Union arc lamps type 300K provided brilliant projected images. The reprojection apparatus is described in detail in reference 15 and the sketch of the projector, Fig. 4, is taken from there.

METHOD OF ANALYSIS OF EVENTS

Because of the large solid angle of observation, the cloud chamber offers possibilities of obtaining more information concerning stars from a pure substance than does any single experimental device. It enables one to study individual events in detail and, with the aid of a stereoscopic camera and projector, it permits reprojection of each track in its original size, shape and position. With the addition of a magnetic field one can gain information about the momentum and energy of each charged particle.

Available Data

Following an outline by J. Tracy,[9] the data available for analyzing an event in this investigation may be divided into three categories. These are:

General Experimental Data. This includes knowledge of the direction and approximate energy distribution of the neutron beam, the direction and strength of the cloud chamber magnetic field, and the composition and stopping power of the gas mixture in the cloud chamber.

Individual Star Data. This includes information obtained from measurements on the individual events, such as initial radius of curvature, density, initial direction, range, rate of change of curvature and rate of change of density.

Auxiliary Information. This includes application of the laws of conservation of momentum, energy, mass and charge, as well as knowledge of range-energy relations, specific ionization vs. energy relations and characteristic track endings.

Identification Procedure

On the average, about 20 oxygen stars appear in each picture and one meson star is obtained for each 95 oxygen stars. The data collection rate is therefore about 1 meson star for each 5 pictures. The negative charge associated with the negative pi meson makes it the only particle associated with a star which has a counter-clockwise curvature in the magnetic field. Electron pairs are created in the gas yielding the only other track with characteristic curvature for a negative particle, but they have no associated star. These tracks lie in a plane

parallel to the chamber bottom and are directed toward the target from which the neutrons come, enabling one to differentiate between mesons and electrons in all cases.

The positive pi mesons and remaining particles of the stars are identified by standard cloud chamber techniques; i.e., by a comparison of Hρ vs. ionization for p, d, t, He^3, and He^4, and by characteristic endings. The heavier short ranged particles could not be identified completely, but in the majority of cases some mass and charge estimate was obtained and when used with range-energy relations for heavier particles[16] gave approximate values for their energy and momentum. The complete identification procedure is outlined in reference 10 and essentially the same procedure was used in the present study.

Stopping Power. The range-energy relations expected from the calculated stopping power of the gas in the chamber were verified experimentally. The energies of protons of range greater than 20 cm. ending in the chamber were determined from Hρ measurements and their ranges measured with a flexible ruler. The calculated and measured ranges agreed within ten percent which is within the experimental error expected. In addition, theoretical track endings were drawn from range-energy relations for the calculated stopping power and compared to the experimental track endings obtained.

Errors in Measurement

Analysis of an event involves, besides identification of the particles, measurements of radius of curvature, dip angle, beam angle, height of track in chamber at point of curvature measurement, length of track used in curvature measurement, distance of track from center of chamber, range (when the track stops in the illuminated region) and magnetic field strength.

Radius of Curvature. The curvature of a track is measured by reprojecting it life-size on a translucent screen adjusted to the proper angles to contain the plane of the track (called the slant plane) (see Fig. 4) and then matching it with one of a series of arcs ruled on a lucite template. The error made in curvature measurement amounts to 0.1 mm error in the sagitta independent of the particular curvature and track length. The effect of turbulence on the curvature can be calculated from

inspection of tracks made with no magnetic field. On the average such errors are negligible in comparison with measurement errors.

Dip Angle and Beam Angle. The accuracy of reprojection and measurement with the apparatus used in this experiment has been investigated by W. Powell and collaborators.[15] They concluded that dip angles α, Fig. 4, could be determined to $\pm 1\,1/2^{\circ}$ for $0^{\circ} < \alpha < 50^{\circ}$ and beam angles β, Fig. 4, to $\pm 1^{\circ}$. The systematic error due to alignment of reference crosses on top glass with the direction of the neutron beam is included in this error. All neutrons are assumed to enter the chamber in a parallel beam and the ratio of the number of stars in the collimated region to the number outside the region makes this a valid assumption.

No restriction of dip angle was placed on measurement of meson events in this study, but for angle and energy distributions the dip angle was limited to $\pm 60^{\circ}$ and proper corrections were made for this limitation. The associated fragments of the stars were identified as completely as possible, and cases in which excessively large dip angles prevented identification of one or more fragments of the star were tabulated only as to the information readily obtainable. The energy involved makes most stars appear swept forward and on the average only the low energy particles are scattered at wide angles. In special cases this is not true, and particles of rather high energy are seen to go off at large angles with respect to the beam direction--some even essentially backward.

Magnetic Field. The ammeter reading of the magnet current is photographed simultaneously with each picture and the field strength is then obtained from a magnetization curve. The magnet field varies by 6 percent over the region where tracks were measured and an accurate map of the field is used to determine the field strength at the center of the measured part of the track. It is necessary to know the magnetic field at the center of a track only since the field varies quite slowly over the useful region of the chamber.

Calculations

The analysis of an event is completed by making appropriate calculations for such quantities as $H\rho$, energy and angle for the particles

of the star, and the minimum energy of the incident neutron. The details for calculating the minimum energy are given in reference 10 and are only briefly outlined here. From the measured dip angle α and beam angle β the scatter angle θ and azimuthal angle ϕ are computed (see Appendix I). The momentum of each particle of the star is then resolved into three components. Momentum components parallel to the beam are added to obtain a forward momentum for an incident neutron. This is not a minimum value for the momentum of the incident neutron because of the possibility of there being neutral particles going backward from the star. The energies of the visible particles of the star, the binding energy of the indicated reaction, and the meson rest mass are added together to obtain a minimum energy for the incident neutron. If the minimum energy and the forward momentum agree and there is no unbalanced transverse momentum, the star is considered balanced. For cases in which this neutron energy and momentum do not agree and the energy balance leads to a larger value for the incident neutron energy than indicated by the momentum balance, a series of approximations is used which involves adding one or more neutron prongs to the star of an energy sufficient to raise the momentum by the required amount.

As a result of the large energy involved in the rest mass of the pi meson, no stars were found for which the momentum balance lead to a larger neutron energy than indicated by the energies of the visible prongs. In about 1/3 of the cases examined the two methods of calculating the minimum incident neutron energy agreed within the limits of experimental error. For these cases very little energy was associated with neutrons leaving the star. 184 stars were treated in this manner, while the remaining stars were measured with the same techniques but no balance was attempted for energy and momentum. The average minimum energy of the incident neutrons producing mesons was 310 Mev.

The absolute minimum threshold for negative pi meson production by neutrons on oxygen calculated by the method of energy and momentum balance (based on the assumption that the entire nucleus acts like a target particle) using the most favorable reaction is 156 Mev.[17] This is much lower than the minimum energy calculated for neutrons producing mesons in this experiment, indicating the nucleon-nucleon character of the interaction.

If one assumes that the $n + n \rightarrow n + p + \pi^-$ excitation function is of the same shape as the $p + p \rightarrow p + n + \pi^+$ excitation function, then it is possible to compare the average value of the incident neutron energy obtained by the energy and momentum balance of the stars with the average value of the energy of the incident neutron indicated by the product of the neutron spectrum[5,11] and the $p + p \rightarrow p + n + \pi^+$ excitation function[17] (see Fig. 12). The details of the average collision producing a meson are given on page 18 and the information concerning the neutron in the nucleus has been used to calculate the relative pion yield. The relative pion yield as a function of the incident neutron energy, curve b, Fig. 12, indicates that the average energy for neutrons producing pions is about 320 Mev. Agreement between this calculated value and the experimental value of 310 Mev is in accord with the predictions of the hypothesis of charge independence of nuclear forces if a deuteron is produced in the n n process. In the sections, Energy and Angular Distributions and Cross Sections, more evidence is given which indicates the charge independence character of nuclear forces.

CORRECTIONS

The relatively low ionization of the mesons makes possible accurate alignment of the tracks up to ± 60 degrees dip angle for all scatter angles. A geometrical correction factor due to the restriction of ± 60 degrees in dip angle was applied to all pion tracks and the tracks at all angles were measured as a check on the validity of this correction so as not to overlook significant contributions at larger angles. The maximum correction factor under these limitations is 1.5 and would apply only to a small group of tracks. In the range $60 \leq \theta \leq 120$ degrees the observed number of tracks for all dip angles was 138 while the number of tracks expected from application of the correction factor to the tracks in the region ± 60 degrees dip angle was 152. The correction factors are shown in Fig. 5 and are determined by the equations given in Appendix V.

RESULTS AND DISCUSSION

Negative Meson Events

The reactions for negative pion production by neutrons on nuclei are

$$n + n \longrightarrow n + p + \pi^- \quad (1)$$

$$\text{or} \quad d + \pi^- \quad (2)$$

$$n + p \longrightarrow p + p + \pi^- \quad (3)$$

The hypothesis of charge independence of nuclear forces[18] would make the n-n interaction the same as the p-p interaction; a reaction which has been studied in some detail.[19, 20, 21, 22, 23] On this basis, reactions (1) and (2) would contribute the majority of the 344 negative pions observed in this study, while reaction (3) would contribute the same number of pions as the reaction ($np \longrightarrow \pi^+ nn$) or about 21 of the 344 observed pions. The possibility of deuteron formation in reaction (2) is of special interest and will be treated in the section on deuteron formation (see page 15).

The events were classified according to the number of prongs displayed on the associated star, not counting the meson track. In addition the events were then classified according to the identity of the fastest associated particle with energy greater than 10 Mev. The results of this classification are given in Table I.

TABLE I

Negative Meson Events
(Energy of Fast Particles Greater Than 10 Mev)

Prongs	Stars	Fast Deuterons	Fast Protons	Unclassified
2	108	39	65	4
3	101	41	49	11
4	77	20	34	23
5	35	5	18	12
6	22	8	10	4
7	1	1	--	--
	344	114	176	54

The interpretation of the second row is as follows: 101 three prong stars were obtained of which 41 showed fast deuterons, 49 fast protons, and 11 were unclassified. Particles of energy greater than 10 Mev are classified as "fast". The unclassified stars in the table arise from events which have no visible particle with energy greater than 10 Mev, or they arise from events whose fastest particle is neither a deuteron or a proton.

If the same classification is made with the restriction that the energy of the fastest particle be greater than 50 Mev, the following tabulation results.

TABLE II

Negative Meson Events
(Energy of Fast Particle Greater Than 50 Mev)

Prongs	Stars	Fast Deuterons	Fast Protons	Unclassified
2	108	15	31	62
3	101	16	29	56
4	77	9	11	57
5	35	5	3	27
6	22	1	2	19
7	1	1	--	--
	344	47	76	221

Deuteron Formation. A coincidence between the positive pion and deuteron was obtained by Crawford, Crowe, and Stevenson[20] which confirmed the formation of deuterons in the free p-p interactions. The data of C. Richman for 340 Mev protons on protons is in agreement with the pion angular distribution required by deuteron formation.[19] For the n-n interaction, deuterons bombarded with neutrons exhibit twice as many events which have a meson, deuteron, and proton as the end products of the reaction producing mesons as events which have no deuteron among the final products.[12]

A comparison of Tables I and II shows no marked change in the ratio of deuterons to protons. The energy spectrum of the deuterons from Table I has no distinct maximum, but rather is spread uniformly over the range zero to 120 Mev with an upper limit at 160 Mev. An analysis of the oxygen stars not containing mesons yielded a deuteron-proton ratio of about 1:3 for particles with energies greater than 50 Mev while the same ratio from Table II is about 3:5. In spite of the difference of these ratios, it is still impossible to be sure that these deuterons are formed directly with the mesons. The stars containing mesons would be expected to exhibit more pick-up deuterons than corresponding stars without mesons because in the former stars the incident neutron has been degraded energetically by meson production to a favorable energy range for the pick-up process. The presence of a large number of energetic deuterons, however, would seem to indicate correspondence between the formation of deuterons and meson production. The fast deuterons obtained from neutrons on oxygen fall into an angular range of ± 30 degrees in θ, which is in agreement with the expected angular distribution of the deuterons from the pion production process; but the pick-up deuterons would have a similarly sharp angular range for high-energy cases, preventing the separation of the two types of deuteron associated with the star.

Positive Meson Events

The reaction for positive pion production by neutrons on nuclei is $n + p \longrightarrow n + n + \pi^+$. The two neutrons in the final state of this reaction are not detectable in a cloud chamber so that the stars associated with positive pion production appear less complex than the stars associated with negative pion production. Only 21 cases of positive pions were found, as compared with 344 negative pions, thus yielding a negative to positive ratio of 16.4 ± 3.7 over all angles and all energies. A determination of this ratio in carbon,[24] using neutrons from a Be target and the emulsion detection technique, yielded a value of 14 to 1. In determining the negative to positive ratio for neutrons on oxygen, it should be noted that the error in the ratio is statistical and no attempt has been made to present the experimental error that might arise from the fact that the positive pion was more difficult to detect than the negative

meson (the positive pion was identified by its relative ionization for a given curvature while the negative pion was identified primarily by its unique counterclockwise curvature).

The positive pions were produced over a wide range of energies and angles, but the small number of events prevented any study of the angular and energy distributions as was done for the negative events. An examination of the associated stars revealed two cases of the fast deuteron in 21 events as compared with the 47 cases in 344 events for the negative pions. If the pick-up process were the predominant process for producing deuterons in the observed cases, the positive pion events with two neutrons in the final state should contribute at least 6 such deuterons instead of the two observed. The evidence is again in favor of some deuteron formation in the production of negative pions in complex nuclei when the final state contains a neutron and a proton.

Energy and Angular Distributions

The distributions for angle and energy have been presented in two frames of reference. The laboratory angular distribution is given in Fig. 7 and the laboratory energy distribution is given in Fig. 8. The general features of the laboratory angular distribution are the same as those obtained for protons on carbon. Measurements by W. Dudziak[22] for 340 Mev protons on carbon at zero degrees and ninety degrees to the beam, and by S. Leonard[25] at 180 degrees to the beam indicate the same forward peak in the production cross section as in the case of neutrons on oxygen. Agreement of the angular distributions of pions produced by protons on carbon and neutrons on oxygen is evidence for the charge independence of nuclear forces. The neutron beam has a continuous energy spread from pion threshold at 280 Mev to a maximum energy of 340 Mev. The result of this spectrum is to furnish a continuous range of meson energies at any viewing angle. For this reason no comparison of the laboratory energy distribution of pions from neutrons on oxygen with the pions from protons on carbon has been made. The average differential cross section over the range zero to 30 degrees has been obtained as a function of the pion energy and is presented in Fig. 11.

There are indications from the data of L. Neher that the production of negative pions by the n-n interaction is similar to the producution of positive pions by the p-p interaction. In order to treat the data obtained here in a way suitable to make a comparison with the p-p data, the problem arises of choosing an appropriate average center of mass for the reaction of neutrons with oxygen. It is assumed that the reaction occurs between a neutron in the nucleus and an incident neutron. Several further assumptions are made, the first being that the nucleons have a gaussian momentum distribution with an average energy of 20 Mev. The second assumption is that the incident neutron (producing pions) has an energy E_1 of 320 Mev. The third assumption is that the cross section for the production process of negative pions is similar in its energy dependence to the cross section for the production of positive pions by protons on protons[26] (Fig. 12, curve c). A marked characteristic of this positive pion cross section is its extremely rapid rise with energy.

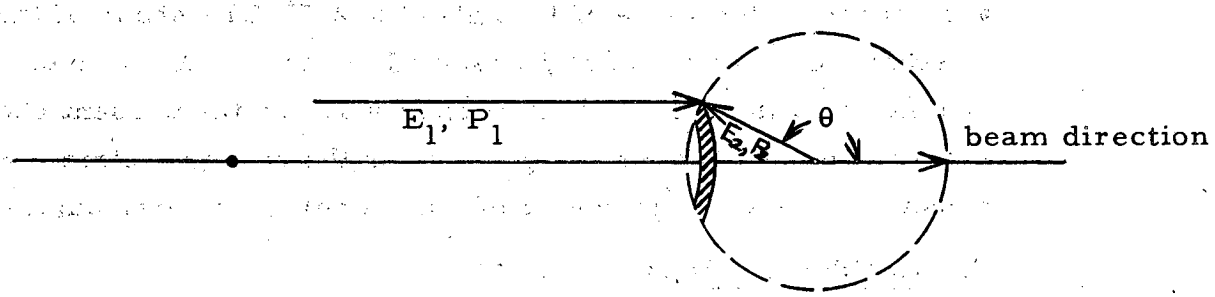

Sketch 1

Sketch 1 shows a schematic representation of the collision of an incident neutron of energy E_1 and a neutron in the nucleus moving at an angle θ to the beam direction with an energy E_2 and a momentum P_2. For a given value of P_2, the energy in the center of mass is a maximum when the angle θ is 180 degrees while the solid angle for collision is a maximum when the angle θ is 90 degrees. Because a rapid rise of cross section with energy has been assumed, the number of negative pions produced becomes a maximum in the region where θ has a value

around 145 degrees. Although the average energy of the neutrons in the nucleus is 20 Mev, the strong energy dependence assumed for the production process makes the most favorable nucleon energy E_2 about 30 Mev.*

Under these assumptions the value β of the average center of mass becomes 0.28 as determined by the relation (see Appendix IV)

$$\beta \cong \frac{CP_1 + CP_2 \cos\theta}{E_1 + E_2}$$

The corresponding value of $\gamma = \frac{1}{\sqrt{1 - \beta^2}}$ is 1.04. The angle and energy of each meson in this average center of mass was obtained by the usual relativistic transformations (see Appendix IV).

Fig. 9 shows the angular distribution obtained for the calculated average center of mass. The uncertainties are the standard deviations based on the number of events observed in 20 degree scatter angle intervals. The solid line in Fig. 9 is a least squares fit of the data to a curve of the type $A(B + \cos^2\theta)$ where B has the value 1.2 with a statistical error of ± 0.15. Richman and Whitehead find that for free p-p collisions the value of B is about 0.2.[31] The shape of the curve is sensitive to the value of β assumed for the center of mass, but the symmetry of the angular distribution justifies the present choice of the average center of mass. Fig. 10 gives the energy distribution of the mesons in the average center of mass over all scatter angles.

The Residual Nucleus

In the case of stars where only a meson, proton and residual nucleus or meson, deuteron and residual nucleus were observed, a special study of the residual nucleus was made. The average recoil range of the residual nucleus was 0.55 ± 0.10 cm representing an energy of 1.5 ± 0.3 Mev.[16] The energy of a neutron, with momentum equal and opposite to the momentum of the recoil nucleus, would be 24 ± 5 Mev. The angle of the residual nucleus recoil is tabulated in 20 degree intervals and the results are given in the following table.

---

*Calculations were performed by L. Neher.

TABLE III

Angular Distribution of the Recoil Nucleus

Angle of Recoil	0-20	20-40	40-60	60-80	80-100
Number of Recoils	55	47	18	5	2

It is clear from Table III that the data concerning the recoil nucleus supports strongly the assumptions made in obtaining the average center of mass.

Cross Sections

Two methods were used to obtain the absolute cross section for the production of negative pions by neutrons on oxygen. The first method used the oxygen stars appearing as background in the chamber and the second method depended on the calibration of an ionization chamber in the neutron beam behind the cloud chamber.

Method I. The cross section for pion production is obtained from the relation

$$\sigma_M = \sigma_i \frac{N_m}{N_s} \qquad (4)$$

where σ_M = cross section for meson production

σ_i = cross section for star production at 310 Mev (inelastic oxygen cross section)

N_m = number of mesons observed

N_s = number of stars produced as background by neutrons above 280 Mev.

The inelastic neutron cross section of oxygen was taken to be 0.7 of the total cross section based on the measurements of W. Ball[5] who determined the ratio of the inelastic to total cross section of carbon, aluminum, copper and lead to be about 0.7 of the total cross section over the range of neutron energies from 100 Mev to 340 Mev. The cross section data for neutrons from 14 Mev to 280 Mev[27] (extrapolated to 340 Mev) was used to obtain curve b Fig. 13 which shows the energy dependence of the total neutron cross section of oxygen. The inelastic cross section is obtained by multiplying curve b by 0.7. The product of the inelastic neutron cross section of oxygen and the neutron energy spectrum from

the LiD target[5,11] is given by curve c, Fig. 13. The area under curve c was divided at 280 Mev into two parts, and the ratio of the shaded area A under the curve for energies above 280 Mev to the total area under the curve was determined to be F (the value of F is about 0.73). In this calculation the number of neutrons below 100 Mev in the LiD spectrum is sufficiently small to be neglected. The product of F and the total number of stars observed is equal to N_s, the number of stars produced by neutrons with energies greater than 280 Mev. The pion cross section calculated from equation (4) is found to be 4.0 ± 1.5 millibarns.

Method II. An independent check on this cross section was obtained by using an ionization chamber behind the cloud chamber to monitor the beam. The neutron pulse associated with a picture passed through the ionization chamber which collected the charged particles produced by the neutrons traversing the ionization chamber. The collected pulse of charge was recorded by a recording electrometer. The relative number of neutrons associated with each picture could be obtained from the recorder trace. To normalize the results of the trace, a similar record was taken during a cloud chamber n-p scattering experiment which used the same target and alignment system[11] with the ionization chamber in the same relative position. By counting the high energy n-p events in the pictures and applying the known cross section for n-p scattering (35 millibarns), the total number of incident neutrons for a series of pictures could be calculated. 156 n-p scatter events, initiated by neutrons above 280 Mev, were counted in 43 pictures. For the same pictures the total trace length was measured from the recorder data, making possible a determination of the average number of neutrons per unit trace length. This result was applied to the oxygen experiment to convert the trace length into an absolute number of neutrons, and the pion cross section was then determined by a straight forward calculation. The value of the cross section obtained by this process if 4.8 ± 1.5 millibarns which is in agreement with the previous result obtained by using the inelastic oxygen cross section.

Errors in the Total Cross Section. The error assigned to the cross section value is made up of the standard deviation based on the number of events and an experimental error based on the extrapolation

for neutron cross sections, the uncertainty in the neutron spectrums and the efficiency of the counting device.

Comparison with Theory

The phenomenological theory of meson production developed by Watson and Brueckner[27] predicts the angular distribution of pions produced in free nucleon-nucleon collisions. They introduce certain simplifications by considering (1) final nucleons in S states only, (2) mesons emitted in P states only, * (3) only pseudoscalar mesons[28, 29, 30] and (4) that conservation laws apply to isotopic spin in addition to parity and angular momentum. The hypothesis of charge independence, contained in the conservation of isotopic spin, can be tested by comparing the results of the neutron bombardment of oxygen from which a study is made of the n-n interaction. The predicted angular distribution for the free nucleon case (in which deuteron formation is assumed, or at least ^3S final nucleons with high probability of deuteron formation) is of the type $A(B + \cos^2 \theta)$ in the center of mass. For 340 Mev protons on protons the value of B is about 0.2, while the theory predicts a value nearer 1/8. For complex nuclei the momentum distribution of the nucleons and the energy spectrum of the beam can be expected to make the distribution more nearly isotropic (the effect would be to smear out the $\cos^2 \theta$ distribution so that it would appear more isotropic in the center of mass). For 340 Mev protons on carbon[22] the value of B is about 0.5, and for neutrons on carbon[7] the value is approximately the same.

The total cross section for the reaction ($nn \longrightarrow \pi^- np$) predicted by the phenomenological theory of Watson and Brueckner is equal to the ($pp \longrightarrow \pi^+ np$) cross section for the same incident energy. In view of the values obtained for protons on carbon by Richman and Wilcox at

---

* 1. For P state emission the reaction ($pp \longrightarrow \pi^o pp$) is forbidden. The small cross section observed for this reaction with respect to the reaction ($pp \longrightarrow \pi^+ d$) is compatible with a dominant P wave term (K. Watson and K. A. Brueckner, P. R. 83, 1 (1951)).

2. The constant angular distribution of the reaction ($pp \longrightarrow \pi^+ d$) with increasing energy of the pion indicates that only one term is important, as the two terms should have different energy dependences (R. Durbin, H. Loar, J. Steinberger, P. R. 84, 581 (1951)).

3. If the pions are restricted to S and P states, the predominantly $\cos^2 \theta$ angular distribution must come from the P wave (M. Whitehead and C. Richman, P. R. 85, 855 (1951)).

90 degrees to the beam[8] and by W. Dudziak at zero degrees to the beam,[22] the cross section for protons on carbon should be about 8.0 millibarns at 340 Mev. Since this value is for 340 Mev protons on carbon it can be expected to be higher than the cross section obtained for neutrons on oxygen because the production process is highly energy dependent.[26] A comparison of the cross section for 340 Mev protons on carbon and the cross section for neutrons on oxygen may be obtained by the application of a correction factor for the energy dependence (the average energy of the neutrons is about 310 Mev instead of 340 Mev as for the proton beam). This reduces the cross section for protons on carbon by a factor of 2.3, so that the values to be compared are 4.4 millibarns for oxygen and 3.4 millibarns for carbon. It thus appears that the efficiency of the production process per nucleon has not changed much from carbon to oxygen and that the estimate of pion production based on the hypothesis of charge independence is in good agreement with experiment.

The phenomenological theory predicts the cross section for the reaction ($pn \longrightarrow \pi^- pp$) to be equal to that for the reaction ($np \longrightarrow \pi^+ nn$). If the experimental value of the cross section for the production of positive pions by protons on carbon is divided by the observed ratio of positive to negative pions, one obtains the expected value of the cross section for the reaction ($pn \longrightarrow \pi^- pp$) and hence an estimate of the expected cross section for the reaction ($np \longrightarrow \pi^+ nn$). From the results of the carbon data[22,24] one would thus expect the positive pion production cross section by neutrons on oxygen to be about 0.76 millibarns (if the neutron beam were monoergic at 340 Mev). When this value is corrected for energy dependence of the production process, a value of 0.33 millibarns is obtained while the observed value for neutrons on oxygen is 0.27 ± 0.1 millibarns. The positive pion cross section for neutrons on oxygen is therefore in agreement with the predictions of charge independence of nuclear forces.

The agreement of the angular distribution and the production cross sections obtained in this study with the angular distribution and cross sections predicted by the phenomenological theory make it appear quite certain that the ideas put foreward by Watson and Brueckner are

in no way contradicted by the data. The relatively large value of the constant term B in the expression for the pion angular distribution in the average center of mass for neutrons on oxygen (B equal to 1.2 as compared with 0.5 for protons on carbon) can be justified without a contradiction of theory. The energy spectrum of the neutron beam contributes an appreciable number of low energy mesons, which would not be present in the case of a monoergic beam or accounted for in calculations that treated only the case of interactions for a fixed incident energy. For this reason it is concluded that the theory has not been contradicted by the data for neutrons on oxygen.

In addition, the observation of a larger number of deuterons in the beam direction in connection with stars showing negative pion production is in agreement with the prediction that the final nucleons in triplet S states have a high probability of forming a deuteron. The ratio of the $\sigma(0^{\circ})/\sigma(18^{\circ})$ (for laboratory angles) furnishes another check on the predictions of the theory of charge independence. On the basis of the production of pions with deuteron formation, the ratio of the cross sections at zero and 18 degrees should be 1.54 (this is the value for the 340 Mev protons on protons) while the experimental value for neutrons on oxygen is 1.6 ± 0.2.

Azimuthal Symmetry Check

Since there is no reason to believe otherwise, all processes in this experiment are expected to occur with azimuthal symmetry. Because this has been one of the assumptions employed in this experiment and in order to be certain that no systematic errors have been made in the angular measurements, a measurement of this symmetry has been made.

The following table shows the number of mesons observed in the four azimuthal angle groups.

TABLE IV

Azimuthal Symmetry Check

Angular Groups	0-60	120-180	180-240	300-360
Mesons	66	78	69	68

These numbers lie well within the errors expected from statistical fluctuations.

Low Energy Mesons

It is possible by the methods outlined in the section on Identification Procedure to identify a meson with an energy as low as 1/4 Mev since it would still have a radius of curvature of one centimeter and would be followed by capture or decay, both of which are observable in a cloud chamber. Few pions of this energy were observed; but one case was obtained where the pion was created and subsequently decayed to a muon and the muon decayed to an electron.

CONCLUSIONS

Among the special types of inelastic events, when oxygen is bombarded by high energy neutrons, are the ones producing pions. These events represent one out of 40 high energy inelastic events and they are easily identified by the distinctive curvature and ionization associated with the event. The negative pions account for all but six percent of the visible meson events. The sharp forward peak of the angular distribution of the negative pions in the laboratory frame is in agreement with the work of other investigators using protons on carbon[22, 25, 31] and also with the work of L. Neher using neutrons on carbon. The conclusion to be drawn from the agreement is the charge independence of nuclear forces. As far as the energy dependence of the process is concerned, no marked dependence is evident since the possible presence of a secondary neutron prohibits an attempt to correlate pion threshold with an incident neutron energy. The energy spectrum contains more low energy pions than found for the case of 340 Mev protons on carbon, which could be expected from the lower energy of the neutrons. The special transformation used for the center of mass distributions is not completely justified but the evidence is quite good that it is not unreasonable. The value of β (0.28) for the transformation is approximately the value taken by other experimenters[7, 21] and the symmetry of the results of its application agrees with the results of experimenters[23] who have made measurements of positive pions from the p-p interaction.

The experiment which remains to be done obviously is the production of negative pions by neutrons on deuterium. This study has been undertaken by W. Powell and M. Knapp[12] and should lead to a clearer picture of the n-n interaction since the calculations become simplified for such an elementary target nucleus. The center of mass transformation can be applied to events to yield angular distributions which will be practically unaffected by scattering, absorption, or similar processes.

ACKNOWLEDGMENTS

The author wishes to express his sincere gratitude to Professor Wilson Powell for suggesting this problem and for his helpful advice and constant encouragement throughout the investigation. The cooperation of many members of the cloud chamber group is also acknowledged with pleasure, and special thanks are due to John De Pangher for supplying a large share of the nomographs used in the calculations. The author has profited greatly from discussions with Professor C. Richman concerning similar work done by the investigators using nuclear emulsions to detect the pions from protons on carbon. The information contained in the transformation problem was kindly supplied by Leland Neher.

APPENDIX I

Definitions

Dip angle α	The angle between the initial direction of the track and its projection on the horizontal plane containing the neutron beam.
Beam angle β	The angle between the projection of the initial track direction on the horizontal plane and the direction of the neutron beam.
Scatter angle θ	The angle between the initial track direction and the neutron beam.
Azimuthal angle ϕ	The angle between the projection of the initial track direction on a plane perpendicular to the neutron beam and the horizontal plane.
Slant radius ρ_s	The radius of curvature of the track measured in the slant plane.
Radius ρ	$\rho = \rho_s \cos \alpha$, and is the radius of curvature which a particle of slant radius ρ_s would have if it were moving with the same momentum in a plane perpendicular to the magnetic field.
Slant Plane	The plane containing the initial track direction and the horizontal line perpendicular to the initial track direction. It is approximately the plane of the track except that in general the path of a charged particle in a magnetic field describes a helix. The slant plane is at dip angle α to the horizontal plane.
Transverse Momentum	$H\rho_t \equiv H\rho \sin \theta$
Momentum in the beam direction	$H\rho_z \equiv H\rho \cos \theta$

APPENDIX II

Sample Pictures

The following pictures serve as examples of the type of events analyzed. The letters are abbreviations for the particle identities. In Fig. 14 the meson event is located centrally in the picture and appears to be a two prong star. Note the negative curvature of the pion track and the density of ionization of the forward track associated with the star in comparison to the background tracks of similar curvature passing through the chamber. This track was identified as a deuteron track caused by a particle of energy 103 Mev scattered at an angle of 11 degrees. The pion was created with an energy of 13 Mev and at an angle of 57 degrees to the beam. The five crosses represent the direction of the beam and are used for stereo-lining up of the pictures. Fig. 14 includes background tracks and additional oxygen stars not producing mesons.

Fig. 15 shows the track of a negative pion created in a five prong star. The letters indicate the identity of the particles causing the tracks. The remaining track was not identified but it is probably a deuteron or triton track from the range-energy relations. Not visible in the picture is another prong that lies along the alpha track and undoubtably carries the remainder of the charge of the oxygen nucleus. The pion making the track shown here had an energy of 74 Mev and was scattered at an angle of 25 degrees. The other particles are low energy and could not possibly lead to a momentum balance for the star. For this reason a secondary neutron is hypothesized which has an energy of at least 40 Mev if it is in the forward direction. Fig. 15 also includes background tracks and additional oxygen stars.

APPENDIX III

Energy and Momentum Relations

The following equations apply to the general case involving any number of neutrons:

$$E_n = \Sigma E_i + \Sigma (B.E.)_i + E_{n'}$$

and

$$P_n = \Sigma P_i \cos \theta_i + \Sigma P_{n'} \cos \theta_{n'}$$

where E_n, P_n = energy and momentum of incident neutron.

ΣE_i = sum of energies of ejected charged particles.

$\Sigma (B.E.)_i$ = sum of binding energies of the particles for the reaction measured.

$E_{n'}$, $P_{n'}$ = energy and momentum associated with a particle of one or more neutron masses, as indicated by the reaction, representing the minimum energy necessary to balance the reaction and leading to the minimum energy possible for the incident neutron.

The final value of the energy and momentum should be made to agree by using proper values for the secondary neutrons that are lumped into the one particle of one or more neutron masses. This case is equivalent to the pd case of reference 10, and the notation is taken from there.

APPENDIX IV

Transformation Equations

The following equations apply to the particular transformation used to obtain the center of mass distribution for the mesons shown in Fig. 8.

$$\tan \theta' = cp_y/cp_x = cp_{y'}/cp_{x'} = \frac{cp \sin \theta}{\gamma (cp \cos \theta - \beta E)}$$

where θ = angle meson track makes with incident neutron direction (scatter angle).

θ' = scatter angle in the center of mass.

E = total energy of meson in lab. frame.

p = momentum of meson in lab. frame.

$\beta = v/c$ for c.m.

$\gamma = 1/\sqrt{1 - \beta^2}$

This equation makes it possible to change the laboratory angular distribution into a center of mass distribution. The transformation of the energy distribution to the center of mass is performed with the aid of the following equation

$$E' = \gamma (-\beta cp \cos \theta + E)$$

where E = energy of the meson in lab. frame.

E' = energy of the meson in c.m. frame.

$\beta = v/c$ for c.m.

θ = scatter angle of meson in lab. frame.

p = momentum of meson in lab. frame.

$$\gamma = \frac{1}{\sqrt{1 - \beta^2}}$$

APPENDIX V

Derivation of Correction Factor

The dip angle a is limited by experiment to any convenient value and the correction factor is then determined by calculating the effect on ϕ. The relation connecting the dip angle, scatter angle and azimuthal angle is

$$\sin a = \sin \theta \sin \phi$$

so $$d\phi = \frac{\cos a \, d a}{\sin \theta \cos \phi} = \frac{\cos a \, d a}{\sin \theta \sqrt{1 - \sin^2 \phi}}$$

let $$x = \frac{\sin a}{\sin \theta} \qquad dx = \frac{\cos a \, d a}{\sin \theta}$$

then $$d\phi = \frac{dx}{\sqrt{1 - x^2}}$$

now $$P(\phi) \, d\phi = \frac{d\phi}{2\pi}$$

and $$P = \int P(\phi) \, d\phi = \int \frac{d\phi}{2\pi} = \frac{1}{2\pi} \int_{x = -\frac{\sin a}{\sin 0}}^{x = +\frac{\sin a}{\sin 0}} \frac{dx}{\sqrt{1 - x^2}} \times 2$$

putting in the limits for the integral

$$P = \frac{2}{\pi} \sin^{-1} \left[\frac{\sin a}{\sin \theta} \right] = \frac{2}{\pi} \times \phi$$

The correction factor is then

$$f = \frac{1}{P} = \frac{\pi}{2} / \phi$$

REFERENCES

1. K. Brueckner and W. Powell, Phys. Rev. 75, 1274 (1949).
2. J. Hadley and H. J. York, Phys. Rev. 80, 345 (1950).
3. D. Kellogg, Thesis, UCRL-1899 (1952).
4. M. Goldberger, Phys. Rev. 74, 1269 (1948).
5. W. Ball, Thesis, UCRL-1938 (1952).
6. W. Hartsough, E. Hayward, and W. Powell, Phys. Rev. 75, 905 (1949).
7. L. Neher, private communication.
8. C. Richman, M. Weissbluth and H. A. Wilcox, Phys. Rev. 85, 161 (1952).
9. J. Tracy and W. Powell, Phys. Rev. 77, 594 (1950).
10. P. Tannenwald, Thesis, UCRL-1767 (1952).
11. J. De Pangher, private communication.
12. W. Powell and M. Knapp, private communication.
13. W. Powell, Rev. Sci. Instr. 20, 402 (1949).
14. W. Powell, UCRL-1191 (1950). (Phys. Rev. in print).
15. K. Brueckner, W. Hartsough, E. Hayward, and W. Powell, Phys. Rev. 75, 555 (1949),
16. Sir E. Rutherford, J. Chadwick, and C. D. Ellis, Radiations from Radioactive Substances, 251 (1951).
17. W. H. Barkas, Phys. Rev. 75, 1109 (1949).
18. K. Watson, Phys. Rev. 85, 852 (1952).
19. K. Watson and C. Richman, Phys. Rev. 83, 1256 (1951).
20. F. S. Crawford, Jr., K. M. Crowe, and M. L. Stevenson, Phys. Rev. 82, 97 (1951).
21. E. Henley, Thesis, UCRL-1467 (1951). See also Phys. Rev. 85, 204 (1952).
22. W. Dudziak, private communication.
23. M. Whitehead, Thesis, UCRL-1828 (1952).
24. H. Bradner, D. J. O'Connell, and B. Rankin, Phys. Rev. (letter) 79, 720 (1950).
25. S. Leonard, private communication.
26. A. G. Schulz, Thesis, UCRL-1756 (1952).
27. Summary of Neutron Cross Section Measurements for 14 Mev to 280 Mev Neutrons; R. Hildebrand, P. Hicks, and W. Harker, UCRL-1305 (1951).

28. K. Watson and K. Brueckner, Phys. Rev. 83, 1 (1951).

29. J. Steinberger, W. K. H. Panofsky, and J. Steller, Phys. Rev. 78, 802 (1950).

30. W. K. H. Panofsky, L. Aamodt, and J. Hadley, Phys. Rev. 81, 564 (1951).

31. C. Richman, private communication.

FIGURE CAPTIONS

Fig. 1 Sketch of the cyclotron, cloud chamber, and collimator arrangement.

Fig. 2 Schematic drawing of 22-inch cloud chamber assembly showing arrangement of magnet, camera and lights.

Fig. 3 Photograph of cloud chamber, magnet and timing circuits. The neutron beam emerges through the hole in the wall and enters the far side of the magnet platform.

Fig. 4 Sketch of the stereoscopic projector used in the life-sized reproduction of tracks. The meanings of the various symbols in the sketch are given in Appendix I.

Fig. 5 Correction factor as a function of the scatter angle. This geometric correction factor corrects for tracks too slanted to be measured. (See Appendix V).

Fig. 6 Incident neutron energy distribution from 340 Mev protons on LiD target. (Reproduced from reference 5).

Fig. 7 Angular distribution of negative pi mesons from neutrons on oxygen. The points were obtained from division of the weighted number of tracks by the average number of steradians in each 20 degree interval. (Laboratory frame). Standard deviations are indicated.

Fig. 8 Energy distribution of negative pi mesons from neutrons on oxygen. The points were obtained by plotting the number of events in each 10 Mev interval. (Laboratory frame). Standard deviations are indicated.

Fig. 9 Angular distribution of negative pi mesons from neutrons on oxygen. The average transformation was applied to the data and the points were obtained from division of the weighted number of tracks by the average number of steradians in each 20 degree interval. (Average center of mass frame). Standard deviations are indicated.

Fig. 10 Energy distribution of negative pi mesons from neutrons on oxygen. The average transformation was applied to the data and the points were obtained by plotting the number of events in each 10 Mev interval. (Average center of mass frame). Standard deviations are indicated.

Fig. 11 Differential cross section $\frac{d^2\sigma}{d\Omega dE}$ for negative pi mesons from neutrons on oxygen. Area under the curve is equal to the average $d\sigma/d\Omega$ for the range $0 \leq \theta \leq 30$ degrees. (Laboratory frame). Standard deviations are indicated.

Fig. 12 Meson yield curve for LiD target obtained from multiplication of LiD neutron spectrum by the p-p excitation function.

Fig. 13 Number of oxygen stars as a function of the incident neutron energy. Curve c is obtained as the product 0.7 x a x b.

Fig. 14 Oxygen star obtained by neutron bombardment showing a deuteron track and a negative pion track. (See Appendix II).

Fig. 15 Oxygen star obtained by neutron bombardment showing tracks due to a proton, deuteron, negative pion and an alpha. The remaining prong was unidentified. (See Appendix II).

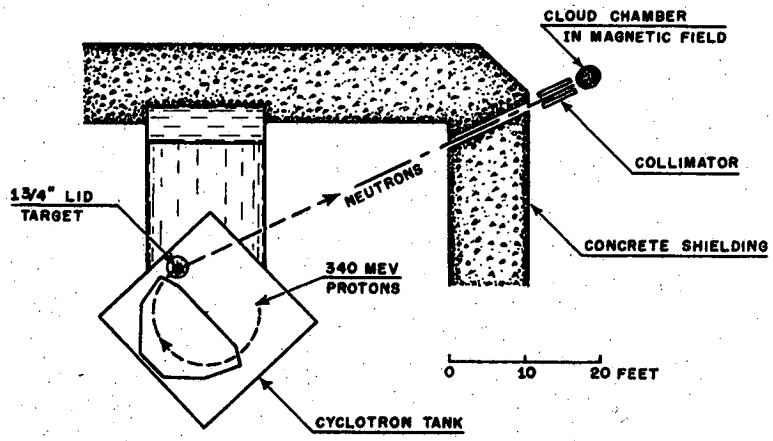
CLOUD CHAMBER
IN MAGNETIC FIELD
COLLIMATOR
NEUTRONS
13/4" LID
TARGET
CONCRETE SHIELDING
340 MEV
PROTONS
0
10
20 FEET
CYCLOTRON TANK

MU-5006

Fig. 1

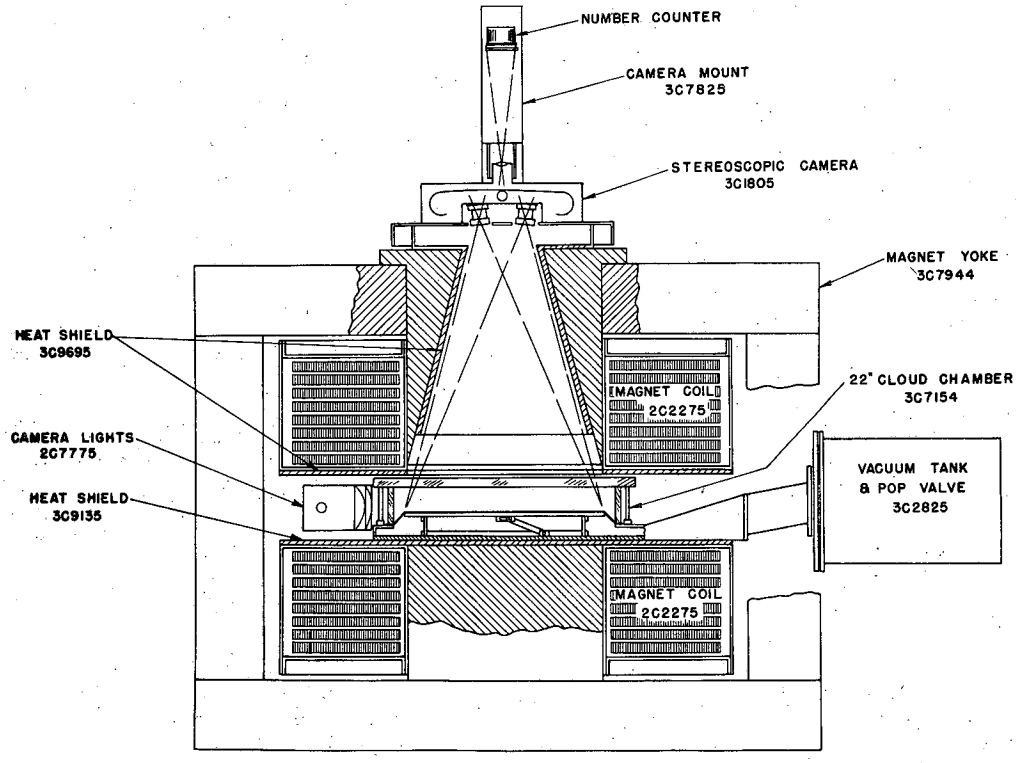

22 CLOUD CHAMBER ASSEMBLY

Fig. 2

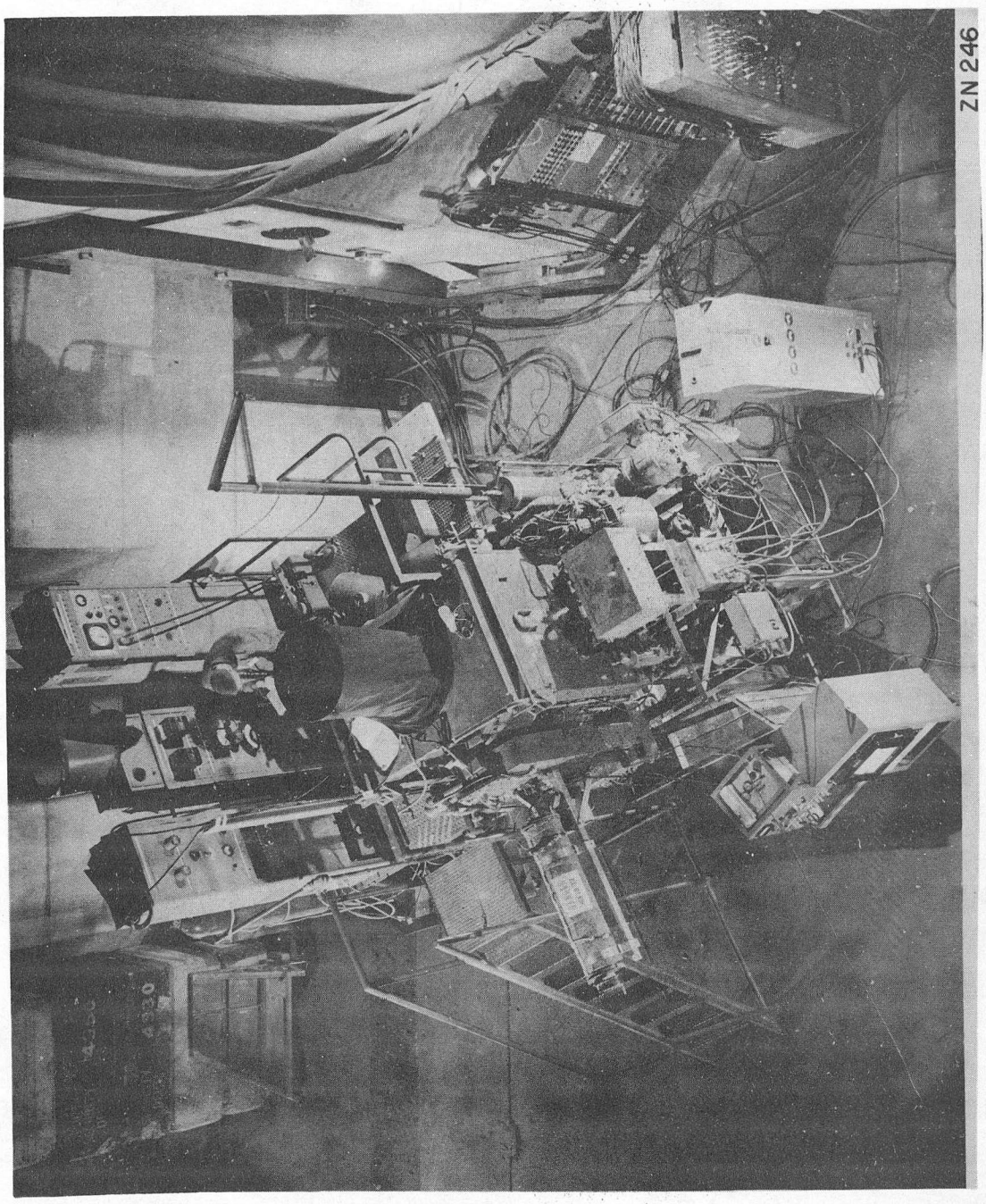

Fig. 3

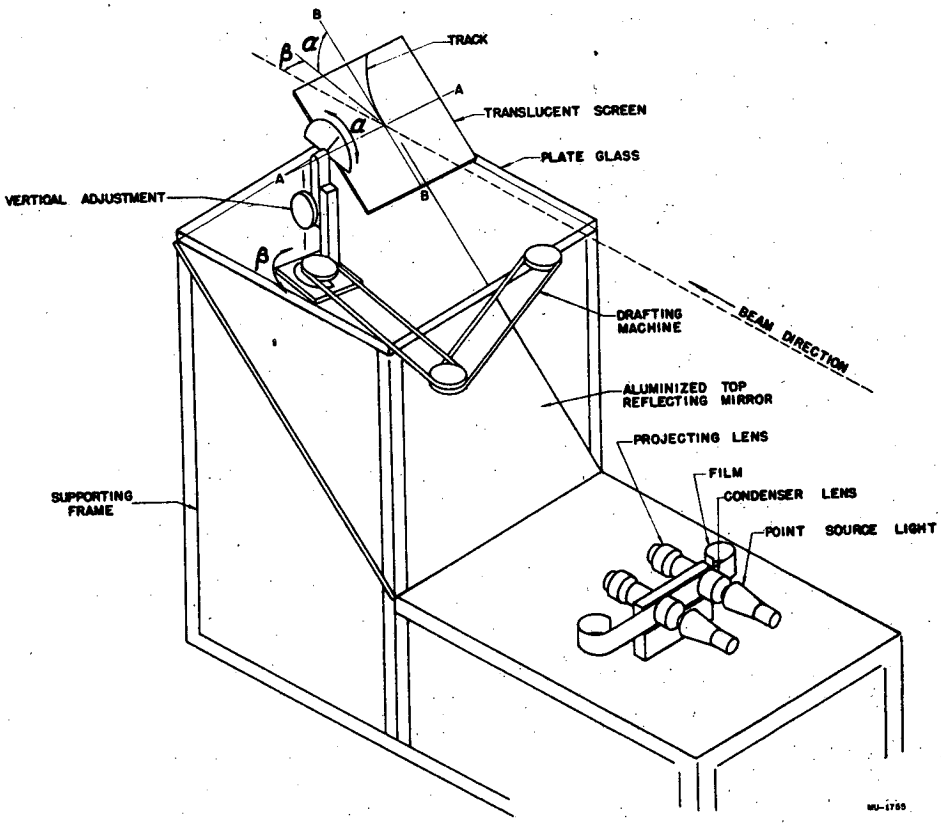
B
β
α
TRACK
A
TRANSLUCENT SCREEN
α
PLATE GLASS
A
VERTICAL ADJUSTMENT
B
β
DRAFTING MACHINE
BEAM DIRECTION
ALUMINIZED TOP REFLECTING MIRROR
PROJECTING LENS
FILM
CONDENSER LENS
SUPPORTING FRAME
POINT SOURCE LIGHT
MU-1755

Fig. 4

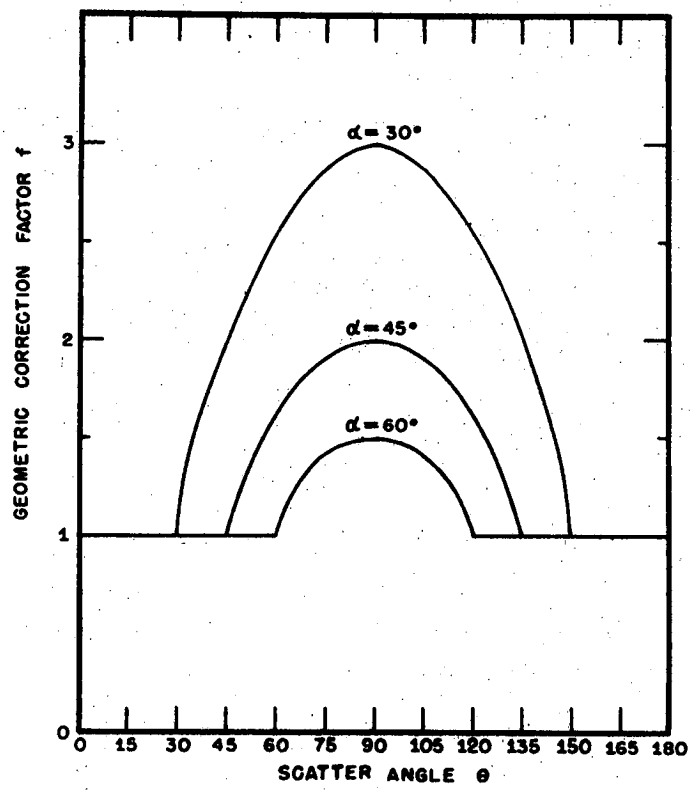

ASSIGN WEIGHT f TO EACH TRACK SEE APPENDIX V

MU-5007

Fig. 5

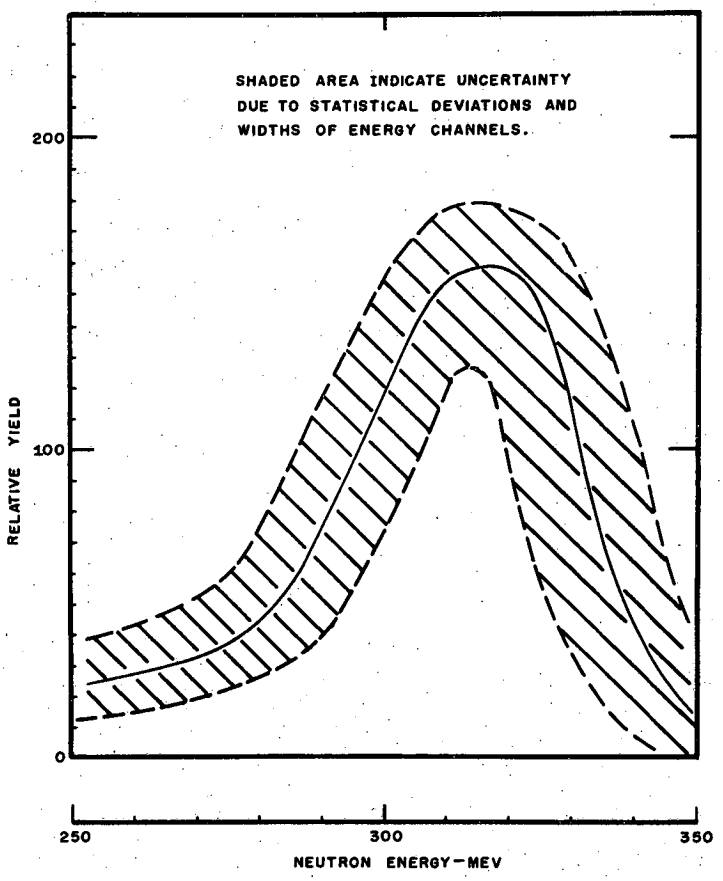

NEUTRON ENERGY SPECTRUM
FROM LID TARGET.

MU-5008

Fig. 6

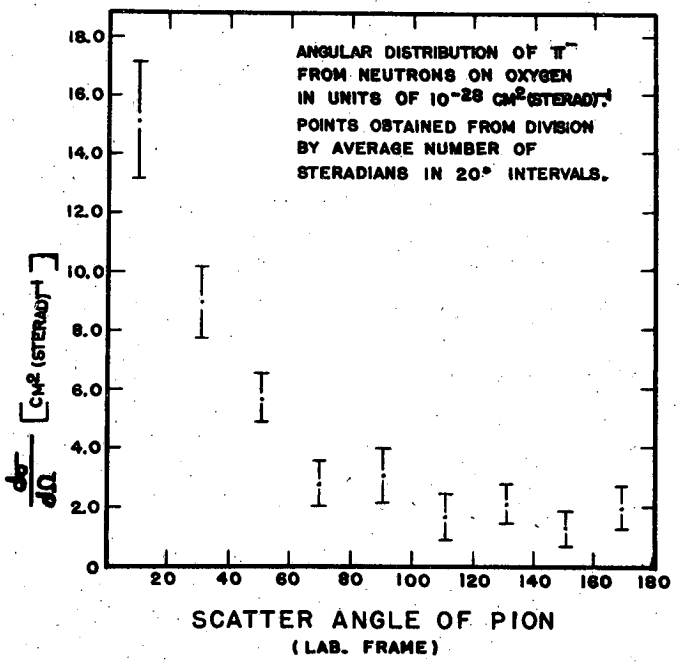
ANGULAR DISTRIBUTION OF π⁻
FROM NEUTRONS ON OXYGEN
IN UNITS OF 10⁻²⁸ CM²(STERAD)⁻¹
POINTS OBTAINED FROM DIVISION
BY AVERAGE NUMBER OF
STERADIANS IN 20° INTERVALS.
dσ/dΩ [CM² (STERAD)⁻¹]
0
2.0
4.0
6.0
8.0
10.0
12.0
14.0
16.0
18.0
20
40
60
80
100
120
140
160
180
SCATTER ANGLE OF PION
(LAB. FRAME)

MU-5009

Fig. 7

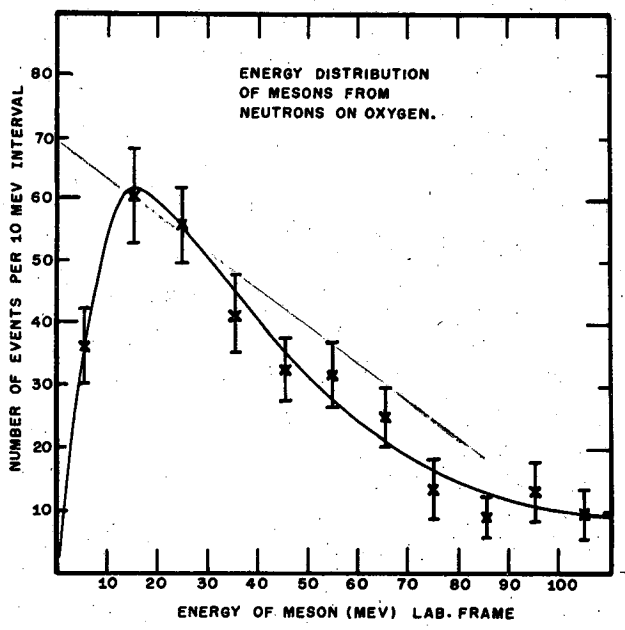
ENERGY DISTRIBUTION
OF MESONS FROM
NEUTRONS ON OXYGEN.
NUMBER OF EVENTS PER 10 MEV INTERVAL
80
70
60
50
40
30
20
10
10 20 30 40 50 60 70 80 90 100
ENERGY OF MESON (MEV) LAB. FRAME

MU-5010

Fig. 8

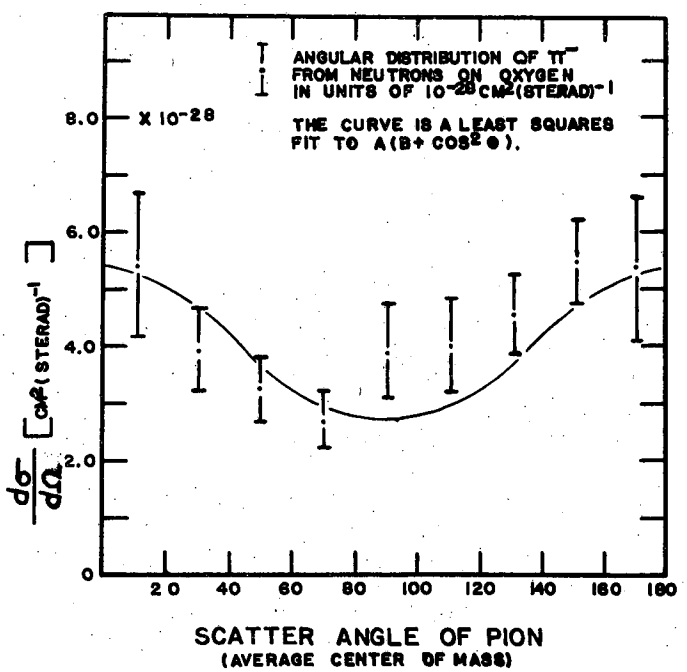
ANGULAR DISTRIBUTION OF π⁻
FROM NEUTRONS ON OXYGEN
IN UNITS OF 10⁻²⁸ CM²(STERAD)⁻¹
THE CURVE IS A LEAST SQUARES
FIT TO A(B+ COS² θ).
X 10⁻²⁸
8.0
6.0
4.0
2.0
0
dσ/dΩ [CM²(STERAD)⁻¹]
20
40
60
80
100
120
140
160
180
SCATTER ANGLE OF PION
(AVERAGE CENTER OF MASS)

MU-5011

Fig. 9

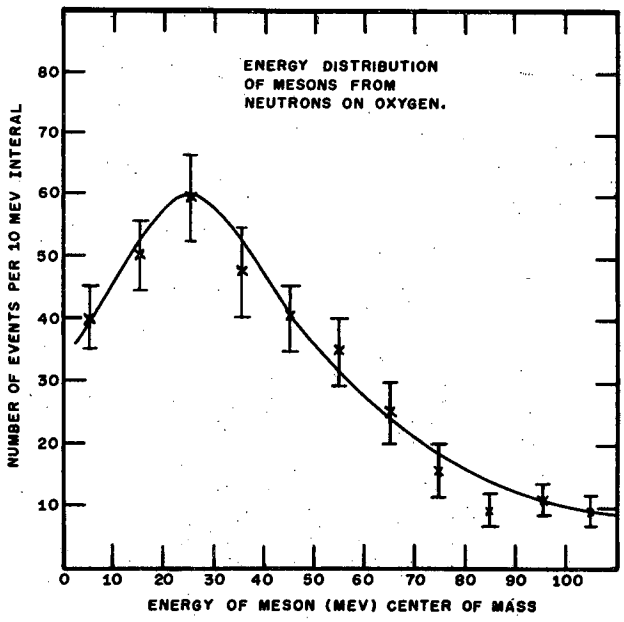

MU-5012

Fig. 10

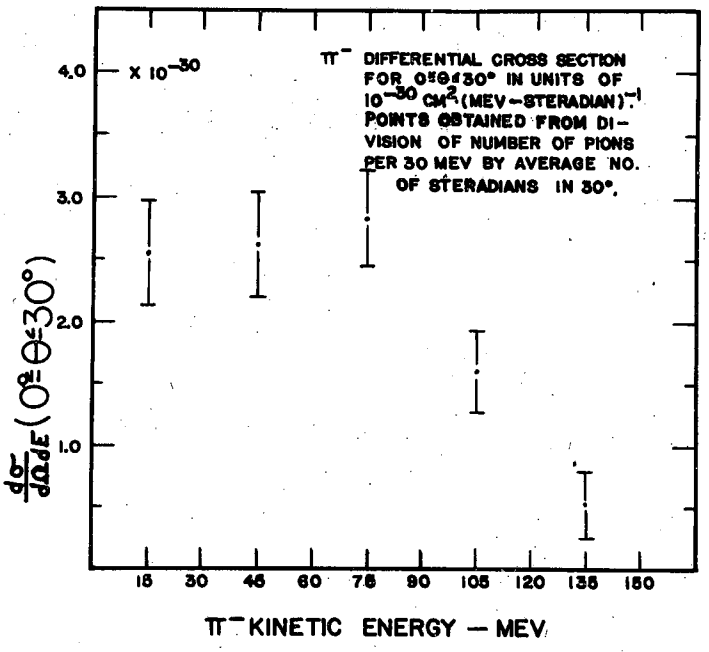
X 10⁻³⁰
π⁻ DIFFERENTIAL CROSS SECTION FOR 0°≤θ≤30° IN UNITS OF 10⁻³⁰ CM²/(MEV-STERADIAN). POINTS OBTAINED FROM DIVISION OF NUMBER OF PIONS PER 30 MEV BY AVERAGE NO. OF STERADIANS IN 30°.
4.0
3.0
2.0
1.0
dσ/dΩdE (0°≤θ≤30°)
15
30
45
60
75
90
105
120
135
150
π⁻ KINETIC ENERGY — MEV
MU-5013

Fig. 11

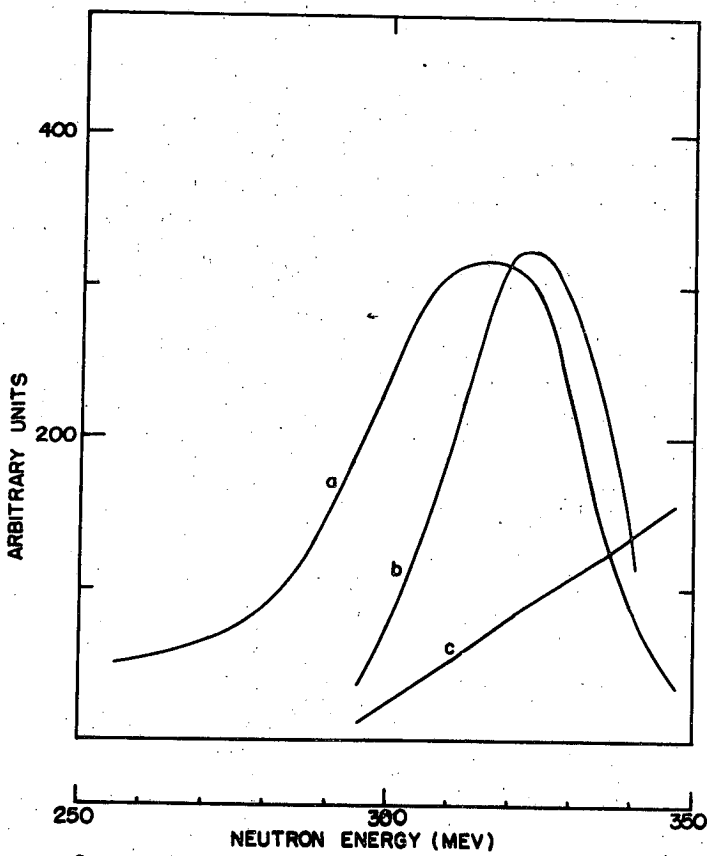

Curve a- Neutron Energy Spectrum From LiD Target
Units- Relative Number Of Neutrons/Mev/Pulse
Curve b- Calculated Meson Yield
Units- Mesons/10^{28}neutrons/nucleus
Curve c- Cross Section For Pion Production For Protons On Protons
Units- 10^{-30} cm^2/Mev

MU-5014

Fig. 12

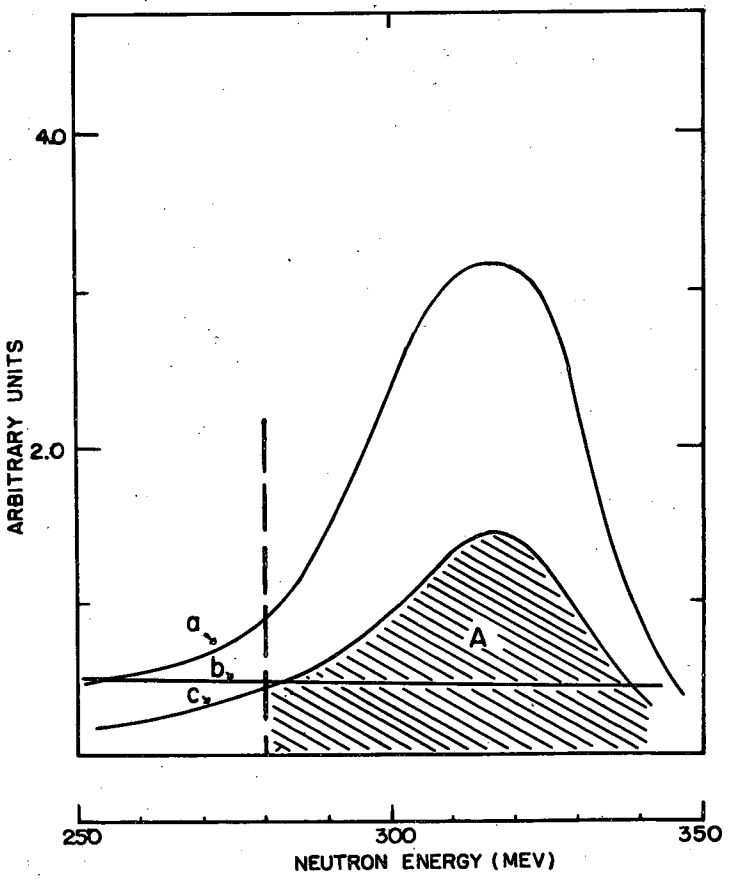

Curve a- Neutron Energy Spectrum From LiD Target
Units- Relative Number Of Neutrons/Mev/Pulse
Curve b- Total Cross Section For Neutrons On Oxygen
Units- Barns
Curve c- Calculated Number Of Oxygen Stars/Mev Obtained as the product 0.7xaxb

MU-5015

Fig. 13

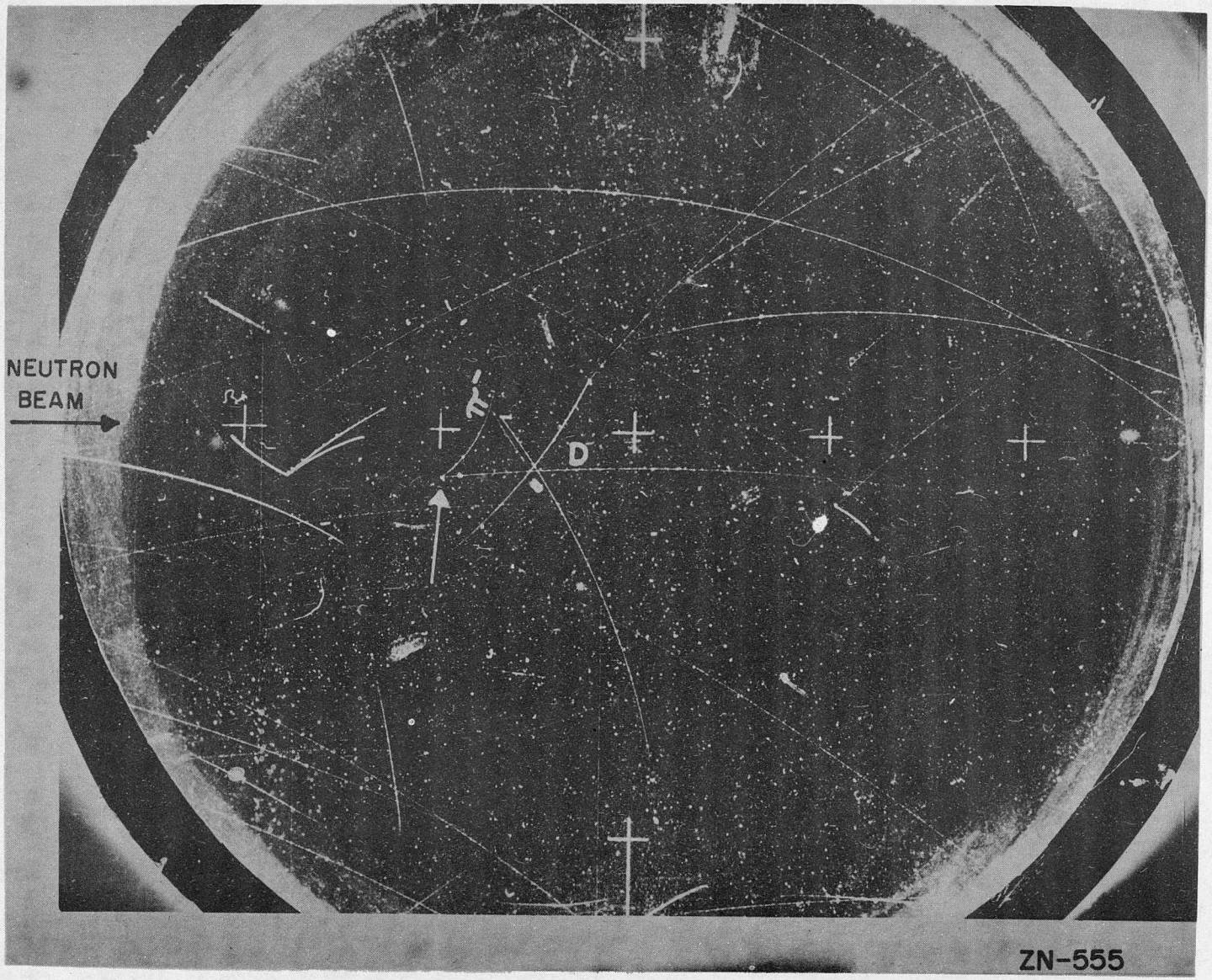

Fig. 14

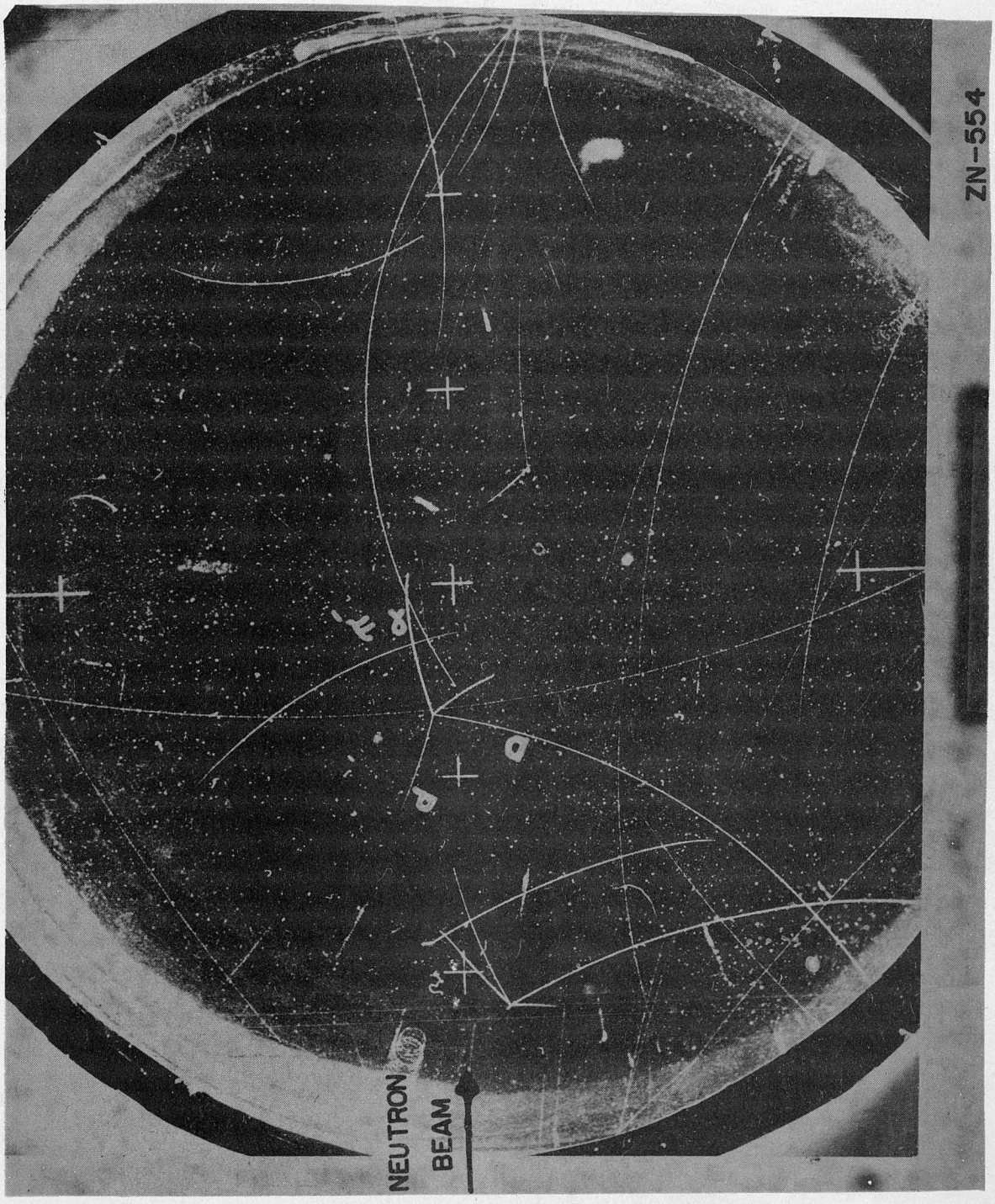

Fig. 15